Since January 2020 Elsevier has created a COVID-19 resource centre with free information in English and Mandarin on the novel coronavirus COVID-19. The COVID-19 resource centre is hosted on Elsevier Connect, the company's public news and information website.

Biocatalysis and Agricultural Biotechnology 32 (2021) 101924

Contents lists available at ScienceDirect

Biocatalysis and Agricultural Biotechnology

journal homepage: http://www.elsevier.com/locate/bab

Molecular dynamics analysis of phytochemicals from *Ageratina adenophora* against COVID-19 main protease (M^{pro}) and human angiotensin-converting enzyme 2 (ACE2)

Netra Prasad Neupane [a,1], Abhishek Kumar Karn [a,1], Imdad Husen Mukeri [a], Prateek Pathak [b], Praveen Kumar [c], Samayaditya Singh [d], Insaf Ahmed Qureshi [d], Tarun Jha [e], Amita Verma [a,*]

[a] *Bioorganic and Medicinal Chemistry Research Laboratory, Department of Pharmaceutical Sciences, Sam Higginbottom University of Agriculture, Technology and Sciences, Allahabad, 211007, India*
[b] *Laboratory of Computational Modeling of Drugs, Higher Medical and Biological School, South Ural State University, Chelyabinsk, Russia*
[c] *Uttar Pradesh University of Medical Sciences, Faculty of Pharmacy, Saifai, UP, 206130, India*
[d] *Department of Biotechnology and Bioinformatics, School of Life Sciences, University of Hyderabad, Hyderabad, 500046, Telangana, India*
[e] *Natural Science Laboratory, Division of Medicinal and Pharmaceutical Chemistry, Department of Pharmaceutical Technology, Jadavpur University, Kolkata, 700032, India*

ARTICLE INFO

Keywords:
Ageratina adenophora
Angiotensin-converting enzyme
Main protease
Molecular docking
COVID-19

ABSTRACT

The outbreak of COVID-19 created unprecedented strain in the healthcare system. Various research revealed that COVID-19 main protease (M^{pro}) and human angiotensin-converting enzyme 2 (ACE2) are responsible for viral replication and entry into the human body, respectively. Blocking the activity of these enzymes gives a potential therapeutic target for the COVID-19. The objective of the study was to explore phytochemicals from *Ageratina adenophora* against SARS-CoV-2 through *in-silico* studies. In this study, 34 phytochemicals of *A. adenophora* were docked with M^{pro} and ACE2 through AutoDock Tools-1.5.6 and their binding affinity was studied. Phytochemicals with higher affinity have been chosen for further molecular dynamics simulations to determine the stability with target protein. Molecular dynamics simulations were studied on GROMACS 5.1.4 version. Furthermore, 5-β-glucosyl-7-demethoxy-encecalin (5GDE) and 2-oxocadinan-3,6(11)-dien-12,7-olide (BODO) were found to be potential blockers with excellent binding affinity with Mpro and ACE2 than their native inhibitors remdesivir and hydroxychloroquine respectively. The drug likeness study and pharmacokinetics of the phytoconstituents present in A. adenophora provide an excellent support for the lead drug discovery against COVID-19.

1. Introduction

Coronavirus disease (COVID-19) caused by the novel coronavirus SARS-CoV-2 and declared as a global pandemic by WHO on March 11, 2020 (Ludwig and Zarbock, 2020; O'Horo, 2020). The first case of COVID-19 was reported in Wuhan, China in december (Tian et al., 2020). The virus is transmitted through direct or indirect contact of the respiratory droplet of an infected person and there is the possibility of air transmission (Brockmeier and Lager 2002; World Health Organization 2020). COVID-19 mainly affects the lungs and requires ventilator support in severe condition (NCT04382391, 2020). Signs and symptoms of infection include fever, dry cough, tiredness, ache and pain, sore throat, conjunctivitis, headache, loss of taste or smell, rash on the skin, or discoloration of fingers or toes (Sahai et al., 2020). SARS, MERS and SARS-CoV-2 belong to the same family, Coronaviridea (Chen et al., 2020). The outbreak SARS has infected 8096 and cause the death of 774 people (Bostancikliogl u 2020) and the MERS infect 2494 people and cause the death of 858 people. The recent outbreak of n-CoV-2 in November 2019, infect 62,686,326 and cause the death of 1,460,387 people globally till November 27, 2020. (Worldometers). The SARS-CoV-2 has a high mortality rate in the elder population, diabetes patients, people having cardiovascular diseases, and lungs diseases (Tskhay et al., 2020). Despite being so dangerous currently, there is no approved vaccine or drug for these viruses. Although hydroxychloroquine, lopinavir-ritonavir, favipiravir, remdesivir, tocilizumab

* Corresponding author. Bioorganic and Medicinal Chemistry Research Laboratory, Department of Pharmaceutical Sciences, Sam Higginbottom University of Agriculture, Technology and Sciences, Allahabad, 211007, India.
E-mail addresses: amitaverma.dr@gmail.com, amita.verma@shiats.edu.in (A. Verma).
[1] Both the authors have equally contributed to the manuscript.

https://doi.org/10.1016/j.bcab.2021.101924
Received 20 October 2020; Received in revised form 19 December 2020; Accepted 19 January 2021
Available online 27 January 2021

Abbreviations

5GDE	5-β-glucosyl-7-demethoxy-encecalin
DAOA	2-deoxo-2-(acetyloxy)-9-oxoageraphorone
OA	9-oxoagerophorone
ODO	(+)-(5R,7S,9R,10S)-2-oxocandinan-3,6(11)-dien-12,7-olide
BODO	(+)-7,7′-bis[(5R,7R,9R,10S)-2-oxocadinan-3,6(11)-dien-12,7-olide
HEDO	(+)-(5R,7S,9R,10S)-7-hydroxy-7,12-epidioxycadinan-3,6(11)-dien-2-one
CED	(−)-(5R,6R,7S,9R,10S)-cadinan-3-ene-6,7-diol
5-CQA	5-O-caffeoylquinic acid
3-CQA	3-O-caffeoylquinic acid
4-CQA	4-O-caffeoylquinic acid
M^{Pro}	COVID-19 main protease
ACE2	Human Angiotensin Converting Enzyme-2
MDPC	methyl 3,4-bis[[(E)-3-(3,4-dihydroxyphenyl)prop-2-enoyl]oxy]-1,5-dihydroxycyclohexane-1-carboxylate
MDCQ	Methyl 3,5-di-O-caffeoyl quinate

are found effective in treating COVID-19 (Neupane et al., 2020)(Lu et al., 2020; Wu et al., 2020). Currently, several types of research and the clinical trial are going on worldwide to find the vaccine, but the success is still far away.

Structurally, SARS-CoV-2 consists of Spike glycoprotein (S), Envelope protein (E), Membrane protein (M), and Nucleocapsid protein (N). Coronaviruses bear positive-sense, single-stranded RNA (+ssRNA) genetic material with approximately 30,000 nucleotides, the longest identified genome in RNA viruses till date (Malik 2020). Viral genome of SARS-CoV-2 consists of 14 open reading frames (ORFs) (Bhosale et al., 2012). Among which the main reading frame ORF1ab encodes for two overlapping polyproteins 1a (pp1a) and replicase polyprotein 1 ab (pp1ab) (Cowley et al., 2000). These polyproteins play a major role in the replication and transcription of the viral genome (Robb et al., 2009). The virus has a protease class of hydrolytic enzyme known as Main protease (M^{pro}) also called as chymotrypsin-like protease (3CLpro). The entry of virus in the host has mediated binding Spike protein with human angiotensin-converting enzyme receptor-2 (ACE2) (Wan et al., 2020). Inside the host cell, proteolytic cleavage of pp1a and pp1ab by SARS-CoV-2 M^{pro} give rise to numerous non-structural proteins like RNA dependent RNA polymerase (RdRp), helicase and non-structural protein 3, 4, and 6 (nsp3, nsp4, and nsp6). These non-structural proteins are thought to be responsible for coronavirus replication. Thus, M^{pro} has emerged as important drug targets (Kirchdoerfer and Ward 2019) and as there is a very low similarity with human proteases and SARS-CoV-2 protease, inhibitors of M^{pro} will be very less toxic to humans. Human angiotensin-converting enzyme-2 (ACE2) is another potential target as it is directly involved in the entry of the virus into the host cell. ACE2 belongs to the angiotensin-converting enzyme family of dipeptidyl carboxydipeptidase. ACE2 protein catalyses the angiotensin I into angiotensin 1-9 and angiotensin II into the angiotensin 1-7. The ACE2 protein is a functional receptor for the spike glycoprotein of coronavirus diseases-2019 (COVID-19). (Magrone et al., 2020; Wan et al., 2020).

A. adenophora (commonly known as Crofton weed) is a perennial, semi-shrubby herbaceous plant which belongs to the Asteraceae family (Zhu et al., 2007). The plant is introduced as an ornamental plant, but leaf extract of the plant is found to have antimicrobial, antiseptic, analgesic, antipyretic, anti-inflammatory, larvicidal, insecticidal, wound healing, antitumor, and also antiviral activity (Poudel et al., 2020). Different research showed leaf extracts of *A. adenophora* have potential anti-viral activity against tobacco mosaic virus (TMV) and Human Immune virus (HIV). Jin et al. investigated antiviral activities of *Eupatorium adenophorum* leaf extract and it inactivated TMV particles and also effective in slight curative as well as preventive purpose (Jin et al., 2014). Ma et al. also suggested that *A. adenophora* has anti-HIV activity(MA et al., 2015). This excited us to do the in-silico screening of *A. adenophora* phytochemical in search of cheaper and less toxic phytochemicals against COVID-19 (André et al., 2019; Jin et al., 2014). Phytochemical screening reported that *A. adenophora* consist various class of secondary metabolites *such as* terpenoids, phenylpropanoids, flavonoids, coumarins, essential oils, sterols, phenolic acids, and alkaloids (Poudel et al., 2020; He et al., 2020). Among all the phytochemicals of *A. adenophora*, 34 phytochemicals were screened and docked with main protease (M^{pro}) of SARS-CoV-2 and angiotensin-converting enzyme receptor-2 (ACE2) of humans and results were compared with standard drugs which are found effective against SARS-CoV-2.

2. Methodology

2.1. Receptor preparation

The crystal structure of a COVID-19 main protease (M^{pro}) and human angiotensin-converting enzyme-2 (ACE2) related carboxypeptidase has been downloaded from protein data bank (PDB) website (http://www.rcsb.org/pdb)(Berman et al., 2000) (PDB ID: 6LU7 and 1R42) and were prepared by using Autodock tools-1.5.6. Kollman charges were added to each atom, non-polar hydrogens were merged, atom types were determined, and the structure of the prepared receptor were saved as pdbqt file.

2.2. Ligand preparation

The list of the major phytochemicals of *A. adenophora* were retrieved from the earlier reported literature (Poudel et al., 2020). The structures of known major chemical components of the plant were prepared using Chemdraw 3D pro12.0. software (Cousins 2005)and built - and - edit module in Open Babel 2.2.3 tool(O'Boyle et al., 2011). MMF F94s force field parameters were assigned to ligands atoms and then the energy has been minimized. Kollman charges were added to each ligand atoms. However, nonpolar hydrogen atoms were merged, and rotatable bonds defined. The structure of the ligands was saved in pdbqt format and used as in put ligand file for Autodock in docking.

2.3. Active site selection

The active site of the COVID-19 M^{pro} protein (PDB ID: 6LU7) and Human ACE2 protein (PDB ID: 1R42) has been predicted from different receptor cavities available. The different active site was identified from Discovery Studio 2020 (BIOVIA) client among these, site 1 of COVID-19 Mpro with coordinates (X = −10.711837, Y = 12.411388 and Z = 68.831286) and ACE2 receptor with coordinates (X = 44.98, Y = 20.98 and Z = 16.80) have been chosen as the active site.

2.4. Virtual molecular docking

The receptor and ligand interaction through virtual molecular docking have been performed through AutoDock Tools-1.5.6. All the molecules have been docked to active site 1 of COVID-19 M^{pro} and active site 1 of ACE2 receptor. Ligand-receptor interaction was viewed through Discovery Studio 2020 Client (BIOVIA) and re-docking of all the compounds was done to assure reproducibility (Pathak et al., 2020).

2.5. Molecular dynamic simulation

The effects of the ligands on the structural dynamics of proteins were studied on GROMACS 5.1.4 version (Abraham et al., 2015). Each complex and apo forms of the M^{pro} and ACE2 proteins were considered for the study. Additionally, the protein and water topology were defined by

GROMOS43A2 force field (van Gunsteren et al., 1996) and SPC/E water model (Berendsen et al., 1987), respectively. Each ligand topology was generated through the same force field using the PRODRG server (http://prodrg2.dyndns.org/submit.html). The charge of each simulating system was neutralized by an appropriate number of sodium ions (Na^+). Subsequently, the energy of the simulating systems was minimized by the steepest descent algorithm in 50,000 steps. The two-phase equilibration of 100ps was carried out by NVT (at constant 300 K) and NPT (at constant 1 bar) ensemble equilibrations for each system. Consequently, MD simulation of 50ns was carried out for each system and the data was used for the enumeration of RMSD, RMSF and Rg. Furthermore, the binding energy was enumerated by the gMMPBSA package (Kumari et al., 2014) of GROMACS for every 0.1 ns frame of the last 20ns simulation of each protein-compound complex.

2.6. Drug likeness property

Physicochemical and pharmacokinetic properties to different phytochemical present in *A. adenophora* were studied using Swiss ADME a free online web tool (Zoete et al., 2016) (http://swissadme.ch/) by submitting their respective structures.

3. Result and discussion

3.1. Virtual screening through molecular docking

The SARS-CoV-2 M^{pro} with N3 inhibitor is divided into three domains. Domain I (from Phe 8 to Try 101), domain II (from Lys 102 to Pro 184) and domain III (from Thr 201 to Val 303). Domain I and II have an anti-parallel β-barrel structure. Domain III contains five α-helices arranged into the large anti-parallel globular cluster and is connected with domain II through loop region, which consist residue from Phe 185 to Ile 200. The substrate-binding site of M^{pro} of SARS-CoV-2 has Cys-His catalytic dyad, where N3 inhibitors bind. This is located in the cleft between domain I and domain II. Fig. 1 represents the crystal structure of COVID-19 main protease (M^{pro}) in complex with an inhibitor N3 and three domains of M^{pro}.

The validation of the docking calculation was evaluated by redocking M^{pro} inhibitor remdesivir on the main protease protein of SARS-CoV-2 (PDB ID: 6LU7). It displayed that remdesivir is able to bind in the almost same pose in the same binding pocket with a binding affinity of −7.8 kcal/mol. The study showed that remdesivir interacts with M^{pro} through various types of interaction with different amino acid residues by making hydrogen bond and Van der Waals bonds. However, it was noticed that the tested ligands interact with Glu A:166, Leu A:141, Gly A:143, Ser A:144, and Cys A:145 amino acids through hydrogen bonds.

The interaction between phyto compound 5GDE and M^{pro} receptor is displayed in Fig. 2.

These interactions are compared with native inhibitor N3 and it was found that 90.90% amino acid showed similarity with that of a co-crystal ligand, which was found acceptable. Thus, the protein was further utilized for docking 34 different compounds reported in *A. adenophora* and docking score is displayed in Table 1 (Poudel et al., 2020).

It was found that among these only three compounds (5GDE, 3-CQA and MDCQ) have better binding affinities than remdesivir. Moreover, 5GDE showed the highest docking affinity (−8.1 kcal/mol) in the entire set of molecules. The comparison between remdesivir and phyto-compound 5GDE complex displayed 100% similarity in interaction pattern, illustrated in Table 2. Among all the interacting amino acids of 3-CQA and MDCQ it was found that 94.11% and 94.73% amino acid interactions are similar with remdesivir, respectively. The docking score along with hydrogen bond and Van der Waals interactions of these three compounds with M^{Pro} is shown in Table 2.

The human ACE2 enzyme is composed of two domains; the first is zinc metallopeptidase domain depicted in Fig. 3(residues 19–611) and the second C terminus domain (residues 612–740). The first domain is 42% identical to the corresponding domains of humans ACE. The first zinc metallopeptidase domain is located near the bottom and on one side of the large active site cleft. The zinc is coordinated by His374, His 378, Glu402 and single water molecules (in the native structure). The second domain is identical to human collectrin by 48%. The ACE2 metallopeptidase domain was divided into two subdomains (I and II), that formed the two sides of a long deep cleft with dimensions of 40 Å long by 15Å wide by 25Å deep. The catalytic subdomains are only connected at the floor of the active site cleft.

Initially, re-docking of the endogenous or native co-crystal ligand has been performed for the validation of the whole docking procedure ensuring its reproducibility. A total of 34 phytochemicals of *A. adenophora* have been docked with human ACE2. The receptor-ligand interactions have indicated that all the compounds used for docking procedure have a substantial binding affinity among them top 5 high scoring compounds are listed in Table 3.

Top 5 high scoring compounds has been taken into consideration for further detailed analysis as reflected in Table 3. BODO has shown the best binding affinity towards the human ACE2 receptor with a binding energy of −8.7 kcal/mol. This binding energy is higher than best fit inhibitor (Hydroxychloroquine) binding affinity, which is −6.3 kcal/

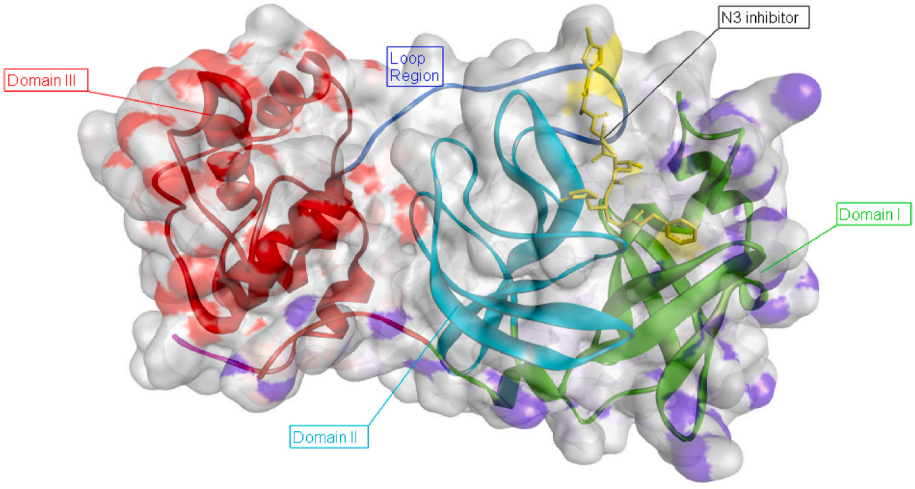

Fig. 1. Crystal structure of COVID-19 main protease (M^{pro}) in complex with an inhibitor N3. Domain I shown in green, Domain II shown in cyan, Domain III is shown in red, and loop region shown in blue. (For interpretation of the references to color in this figure legend, the reader is referred to the Web version of this article.)

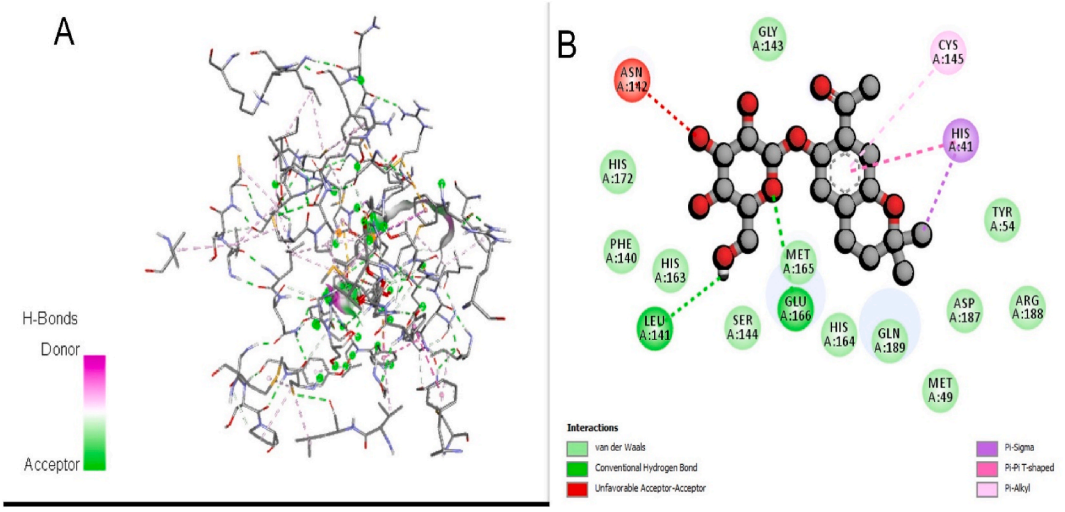

Fig. 2. (A) The phytocompound 5GDE M^{pro} complex. (B) Detail amino acid interaction of 5GDE complex with M^{pro} in 2D.

mol. The best fit inhibitor was selected by comparing binding affinity of several drugs that have shown activity against COVID-19. The interaction of the compound with the human ACE2 receptor is depicted in Fig. 4. Docking study has exhibited that BODO interacts with 11 amino acid residue among which 7 residues (GLU A:495, ASP A:494, PRO A:492, HIS A:493, TRP A:478, TYR A:613, GLUA:489) matches with that to the inhibitor hydroxychloroquine. Thus, can be predicted compound binds to the receptor properly to inhibit human ACE2 protein.

MDPC, a phytochemical of *A. adenophora,* has shown a binding energy score of −7.5 kcal/mol, which is higher than the native inhibitor. The study stated that MDPC interacted with 10 amino acid residues (TYR A:613, ARG A:482, GLU A:489, ASP A:494, ASP A:471, HIS A:493, TRP A:478, GLN A:472, GLU A:495 and GLU A:479), which matches with the hydroxychloroquine. Further, it was also noticed that 5GDE have higher binding affinity (−6.7 kcal/mol) with human ACE2 than native inhibitor hydroxychloroquine. Additionally, the careful study of interaction emphasized that the compound 5GDE interacts with two amino acids through hydrogen and pi-alkyl bonds, where one amino acid residue HIS A: 493 found common to the native hydroxychloroquine.

A. adenophora phytochemical have already proven anti-TMV and anti-HIV activity. In our in-silico study molecular dynamics of phytochemicals of *A. adenophora* done with M^{pro} and ACE2 virtually and found that phytochemicals BODO and 5GDE, were potential blockers of M^{pro} and ACE2. These plant materials are extremely abundant, convenient to harvest and easy to collect. This will lead to cost effective drug can be develop.

3.2. Molecular dynamic simulation

To elucidate the effects of the selected compounds (BODO and 5GDE) on the structural attributes of the respective protein (ACE2 and M^{pro}), the comparative MD analysis was carried out between each protein complex and its apo form. The average RMSD of M^{pro} complex and apo form was enumerated as 0.37, and 0.29 nm, wherein M^{pro} exhibited low deviations in backbone atoms with 5GDE in comparison to the apo structure. The RMSD graph is displayed in Fig. 5.

Further, the effect of interaction between compound and M^{pro} protein on its compactness was analyzed by Rg analysis. The respective average Rg values were computed as 2.14 and 2.15 nm for apo and complex form, suggesting that both forms exhibited a similar level of compactness during simulation. The backbone atom fluctuation of the M^{pro} residues in both forms was analyzed by the RMSF data, which showed that apo and complex form have an average RMSF of 0.21and 0.15 nm, respectively. It indicates that backbone atoms of M^{pro} residues showed low fluctuation in complex form in comparison to the apo form. The MD analysis showed that the M^{pro} complex structure retains similar compactness like its apo structure, but with increased structural stability and low residue fluctuation in comparison to the apo form during the simulation. Analysis also depicts the stability of interactions between 5-β-glucosyl-7-demethoxy-encecalinand protein during the dynamics. Simultaneously, the average RMSD of the respectiveACE2 complex and apo form was enumerated as 0.34, and 0.25 nm that delineate lesser deviations in the backbone atoms of the ACE2-compound complex in comparison to its apo structure. The effect on compactness of the ACE2 after accommodating the BODO was analyzed through Rg analysis. The average Rg value for the ACE2 apo and complex form was found to be 2.47 and 2.46 nm, respectively, indicating that both apo and complex forms of ACE2 protein attained a similar level of compactness. The Rg graph is displayed in Fig. 6.

The backbone atom fluctuation of the ACE2 residues was analyzed by the RMSF data, which showed similar levels of fluctuation in apo and complex forms with an average RMSF of 0.15 and 0.14 nm, respectively. The MD analysis showed that the ACE2 complex structure retains similar compactness and residues motion like its apo structure, but with increased structural stability during the simulation. The RMSF graph is displayed in Fig. 7.

In addition, the interface affinity of the protein and compound was analyzed by calculating the binding energy of the protein complex. The average binding energy calculated for ACE2 (BODO) and M^{pro}-(5GDE) complex is presented in Table 4 which represents that Van der Waals energy played a major role in maintaining the binding of compounds with protein in both of the complexes during the dynamics.

Drug likeness is a crucial step in the initial step of drug discovery. The pharmacological properties of 4 high scoring phytochemicals of *A. adenophora* were studied. The pharmacokinetics profiling and toxicity predictions need to assess its drug-likeness property using Swiss ADME, which works on interpreting the molecular fingerprint of the submitted query structure, and analyze the presence or absence of chemical features in a molecule to publish pharmacokinetic data. The *in silico* pharmacokinetic predictions of the top 10 compounds of *A. adenophora* are depicted in Table 5.

MW: Molecular Weight, n-rotb: Number of rotable bonds, n-HbA: Number of hydrogen bond acceptor, n-HbD: Number of hydrogen bond donors.

Four compounds depicted in the table are high scoring compounds in 2 different receptors ACE2 and M^{pro} but BODO and 5GDE are the top-scoring compounds, respectively. These compounds also have single

Table 1
Docking score of 34 phytochemicals present in *A. Adenophora* with Main protease protein (M^{pro}) and human ACE2.

S. N	Phytochemicals	Docking score of M^{pro} (affinity Kcal/mol)	Docking score of human ACE2 (affinity Kcal/mol)
1	7-hydroxy-dehydrotremetone	-6.3	-5.7
2	7,10,11-trihydroxy dehydrotremetone	-6.6	-6.2
3	10-oxo-7-hydroxy-nordehydrotremetone	-6.2	-5.7
4	2αmethoxyl-3β-methyl-6-(acetyl-O-methyl)-2,3-dihydrobenzofuran	-5.7	-5.3
5	5-b-glucosyl-7-demethoxy-encecalin (5GDE)	-8.1	-6.5
6	8-hydroxy-8-b-glucosyl-2-carene	-6.6	-5.7
7	(4S,4aR,6R)-1-acetyl-6-(acetyloxy)-4,4a,5,6-tetrahydro-4,7-dimethylnaphthalen-2(3H)-one	-6.6	-5.7
8	2-deoxo-2-(acetyloxy)-9-oxoageraphorone(DAOA)	-6.2	-6.0
9	9-oxoagerophorone(OA)	-5.9	-5.3
10	9-oxo-10,11-dehydro-agerophorone (ODA)	-6.0	-5.9
11	9β-hydroxy-ageraphorone	-5.8	-5.4
12	Muurol-4-en-7-ol	-5.7	-5.5
13	8-beta-hydroxy-9,12-dehydroverbocciolenten	-5.5	-5.2
14	2 β-acetoxy-(7α, 9β H)-3.6(11)-cadinadien-12(7)-olide	-6.9	-6.4
15	3-hydroxymuurola-4,7 (11)- dien-8-one	-6.1	-5.5
16	(+)-(5R,7S,9R,10S)-2-oxocandinan-3,6(11)-dien-12,7-olide (ODO)	-6.8	-6.5
17	(+)-7,7′-bis[(5R,7R,9R,10S)-2-oxocadinan-3,6(11)-dien-12,7-olide (BODO) (He et al., 2008)	-6.3	-8.8
18	(+)-(5R,7S,9R,10S)-7-hydroxy-7,12-epidioxycadinan-3,6(11)-dien-2-one (HEDO)	-6.7	-6.3
19	(−)-(5R,6R,7S,9R,10S)-cadinan-3-ene-6,7-diol (CED)	-5.8	-5.5
20	(+)-(5S*,6R*,9R*,10S*)-5,6-dihydroxycandinan-3-ene-2,7-dionel	-6.0	-5.7
21	7-hydroxycandinan-3-ene-2-one	-5.6	-5.4
22	5,6-dihydroxy candinan-3-ene-2,7-dione	-6.5	-5.9
23	2-acetyl-candinan-3,6-diene-7-one	-6.1	-6.1
24	Candinan-3-ene-2,7-dione	-5.8	-5.3
25	Candinan-3,6-diene-2,7-dione	-6.2	-5.6
26	1,6-dihydroxy-1-isopropyl-4,7-dimethyl-3,4dihydronaphthalen-2 (1H)-one	-6.4	-5.8
27	(4R,5S)-4-Hydroxy-5-isopropyl-2-methyl-2-cyclohexehone	-4.9	-4.6
28	5-O-caffeoylquinic acid (5-CQA)	-7.2	-6.3
29	3-O-caffeoylquinic acid (3-CQA)	-8.0	-6.4
30	4-O-caffeoylquinic acid (4-CQA)	-7.6	-6.4
31	5-O-trans-o-coumaroylquinic acid methyl ester	-7.0	-6.3
32	methyl (1*R*,3*S*,4*S*,5*S*)-3-[(*E*)-3-(3,4-dihydroxyphenyl)prop-2-enoyl]oxy-1,4,5-trihydroxycyclohexane-1-carboxylate	-7.3	-6.2
33	methyl 3,4-bis[[(*E*)-3-(3,4-dihydroxyphenyl)prop-2-enoyl]oxy]-1,5-dihydroxycyclohexane-1-carboxylate (MDPC)	-7.4	-7.3
34	Methyl 3,5-di-O-caffeoyl quinate (MDCQ)	-8.0	-6.8

lead likeness violations. Therefore, these molecules can be considered for the further drug development steps. Among these two 5GDE has a molecular weight less than 500, which follow Lipinski's rule of five. This can propound that the compounds are safer and permissible for further study. The computational activity predication for expressed that

Table 2
Molecular interaction of top 3 high scoring compounds with Main protease protein (M^{pro}) of SARS-CoV-2.

S. N.	Compounds	H-bond interactions	Van der waals interactions
1.	5GDE	LEU A:141, GLU A: 166	MET A:49, TRY A:54, ARG A:188, ASP A:187, GLN A:189, SER A:144, MET A:165, SER A:144, HIS A:163, PHE A:140, HIS A:172, GLY A:143
2.	3-CQA	GLU A: 166, CYS A: 145, THR A: 190	HIS A:172, PHE A:140, LEU A:141, ASN A:142, SER A:144, GLN A:189, ARG A:188, GLN A:192, ALA A:191, PRO A:168, HIS A:164
3	MDCQ	LEU A:141, HIS A:163, SER A:144, SER A:144, GLN A:192	PHE A:140, ASN A:142, GLY A:143 TRY A:54, ASP A:187, ARG A:188, GLN A:189, THR A: 190, LEU A:167, GLN A: 166

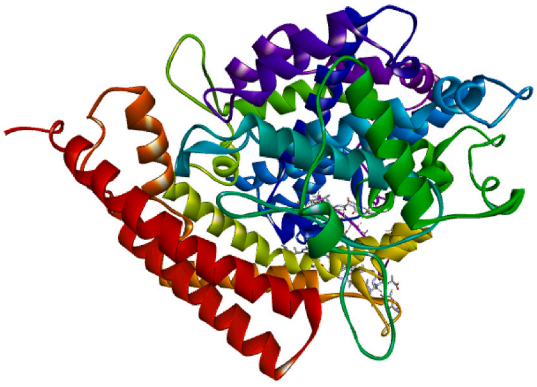

Fig. 3. The crystal structure of COVID-19 zinc metallopeptidase domain of ACE2 (PDB ID: 1R42). Surface is created around the co-crystal ligand present in the binding pocket in which docking is performed for the study.

Table 3
Enlisting of molecular interactions of top 5 high scoring *A. adenophora* phytochemical with human ACE2 protein.

S. N.	Compound Name	Hydrogen bond	Van der Waals interaction
1	BODO	-	UNK C:909, PRO A: 492, TYR A:613, GLU A:495, GLU A:489, TRP A: 478, HIS A: 493, ASP A:494, LYS A:475, UNK C:907, MET A:474
2	MDPC	TYR A:613, ARG A:482, ASP A:471, GLU A:489	UNK C:910, UNK C:909, ASP A:615, SER A:611, ASP A:609, ASP A:494, HIS A:493, GLN A:472, TRP A:478
3	5GDE	HIS A:493	-
4	ODO	ARG A:482	TRP A:478, PRO A:492, GLU A:489, THR A:608
5	MDCQ	HIS A:493, GLU A:479	SER A:611, ALA A:614, TYR A:613, UNK C:909, ARG A:482, TRP A:478, UNK C:908, UNK C:907, MET A:474, ASP A:494

selected phyto-compounds have mild to moderate potency against COVID-19 proteins.

3.3. Probable mechanism of action

The coronavirus is positive-strand RNA viruses (Weiss and Navas-Martin 2005). The process of viral replication and transcription is

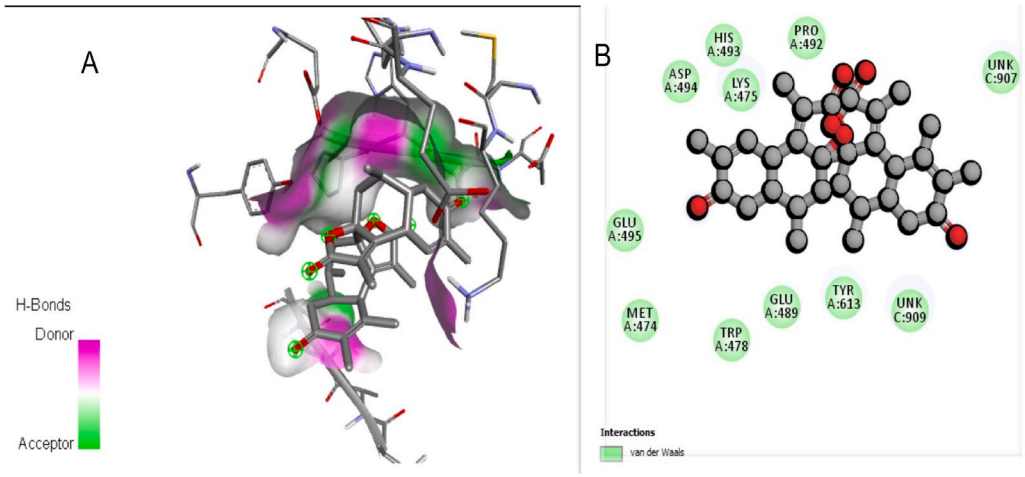

Fig. 4. (A) The phytocompound BODO ACE2 complex. (B) Detail amino acid interaction of BODO with ACE2 receptor in 2D.

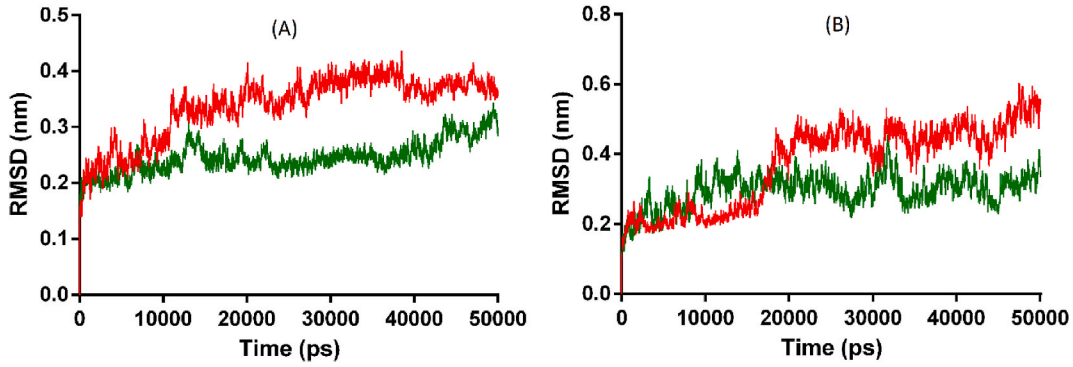

Fig. 5. A and B displayed RMSD of ACE2 and M^{pro}.

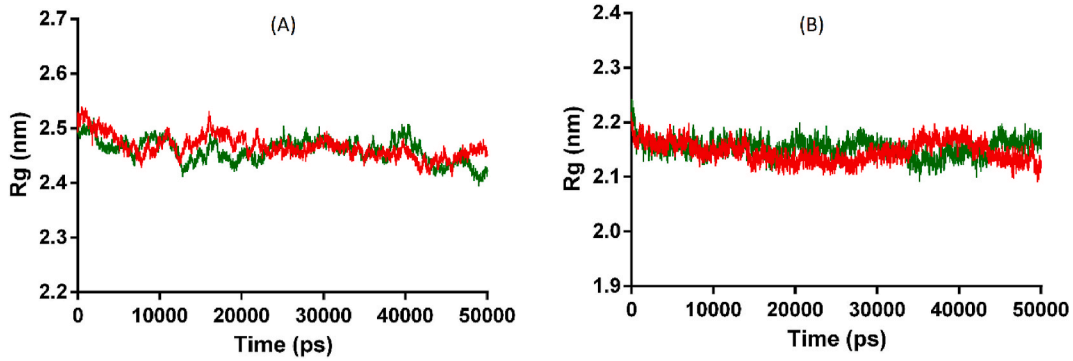

Fig. 6. (A) and (B) displayed Rg of ACE2 and M^{pro}.

controlled by two overlapping polyproteins, the pp1a (replicase 1a, 450KD) and pp1ab (replicase 1 ab, 750KD) (Yang et al., 2003). Frame shifting of the ribosome is essential for the expression of the C-proximal of pp1ab polyprotein (Kjær and Belsham 2018). The release of functional polypeptides from both polyproteins is controlled by M^{pro}, and necessary for proteolytic processing of polyproteins translated from viral RNA. The main protease slices the polyprotein by autolytic cleavage of the enzymes. This indicates blocking the activity of the main proteases could lead to inhibition of viral replication 5GDE, inhibits the M^{pro} with more binding affinity than native inhibitor through the multiple types of interactions.

Coronavirus also presents on protein S a specific binding site for ACE2 which serves as an entry point into the host cell. Various researches on ACE2 suggest, blocking the ACE2 receptor could make it more difficult for coronavirus to enter cells. BODO binds to the ACE2 receptor more effectively with higher binding affinity and most of the amino acid residue (GLU A:495, ASP A:494, PRO A:492, HIS A:493, TRP A:478, TYR A:613, GLUA:489) matches with native inhibitor hydroxychloroquine. 5GDE and BODO are phytochemicals of *A. adenophora* inhibit the viral replication and block the entry of SARS-CoV-2 through M^{pro} and ACE2 receptors. Phytochemicals of these two *A. adenophora* phytochemicals have shown more effective binding energy than its native inhibitors remdesivir and hydroxychloroquine.

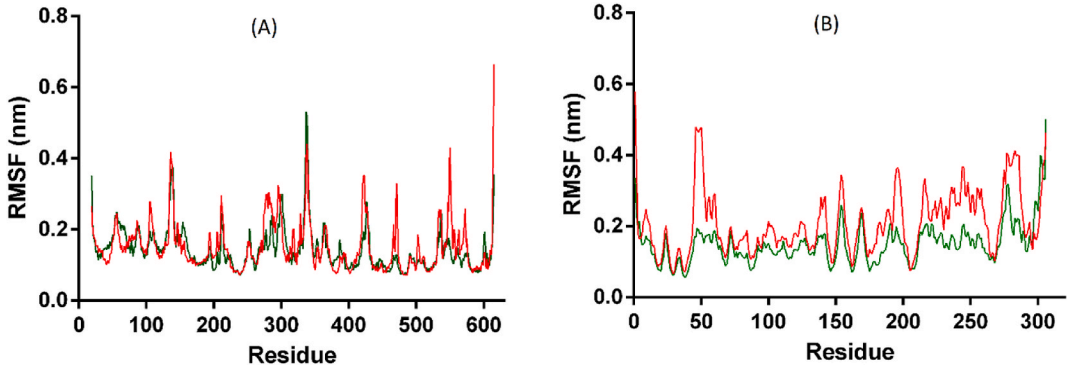

Fig. 7. (A) and (B) displayed RMSF of ACE2 and M^{pro}.

Table 4
The Binding energy of the protein-compound complex. Drug likeness property.

Complex	Van der Waal energy (Kj/mol)	Electrostatic energy (Kj/mol)	Polar salvation energy(Kj/mol)	SASA energy (Kj/mol)	Binding energy (Kj/mol)
ACE2-Comp	-181.67 ± 0.97	-7.39 ± 0.62	98.33 ± 1.51	-15.75 ± 0.08	-106.52 ± 1.33
M^{pro}-Comp	-166.48 ± 0.82	-40.96 ± 0.65	108.23 ± 0.89	-17.03 ± 0.074	-116.31 ± 0.89

Table 5
In silico pharmacokinetics prediction (Lipinski parameters) for the top 4 phytochemicals of *A. adenophora*.

Pharmacological properties	*BODO*	*5GDE*	*MDCQ*	*MDPC*
MW	504.61	382.40	532.49	516.49
n-rotb	1	4	11	10
n-HbA	6	8	12	11
n-HbD	0	4	6	6
ILog P	3.12	2.45	2.92	2.39
Lipinski violations	1	0	3	3
Lead likeness violations	1	1	2	2

4. Conclusion

Our aim of the study was to investigate efficiency of the phytocompounds against coronavirus. Therefore, the phytochemicals of *A. adenophora* are *in-silico* tested against M^{pro} and ACE2 receptor. Furthermore, the docking calculation confirmed that the phytocompound 5GDE consist significant identical interaction with selected protein as referenced compounds. However, the binding energy was measure slightly above than standard drug remdisivir and hydroxychloroquine. The MD analysis of M^{pro} complex structure found to retain similar compactness like its apo structure, but with increased structural stability and low residues fluctuation in comparison to the apo form during the simulation. Whereas, phytochemical BODO has shown high binding affinity (score), almost stable interaction with ACE2 receptor, retain similar compactness, and residues motion like its apo structure, but with increased structural stability during the simulation.

Our study showed natural compounds from *A. adenophora* have either similar or greater binding affinity than that of natural inhibitor remdesivir and hydroxychloroquine. Hence, 5GDE and BODO can be further developed as drug candidates against M^{pro} and ACE2 receptor of coronavirus, responsible for ongoing pandemic. Finally, we suggest from this *in-silico* study that *A. adenophora* phytochemicals block both M^{pro} and ACE2 receptors.

Declaration of competing interest

Authors have no conflict of interest regarding this article.

Acknowledgements

The authors are very grateful to the Department of Biotechnology and Bioinformatics, School of Life Sciences, University of Hyderabad, Hyderabad, Telangana, India. Prateek Pathak acknowledged that the work was supported by Government of the Russian Federation, contract 02. A03.21.0011.

References

André, R., Catarro, J., Freitas, D., Pacheco, R., Oliveira, M.C., Serralheiro, M.L., Falé, P. L., 2019. Action of euptox A from Ageratina adenophora juice on human cell lines: a top- down study using FTIR spectroscopy and protein profiling. Toxicol. Vitro 57, 217–225.

Berman, H.M., Westbrook, J., Feng, Z., Gilliland, G., Bhat, T.N., Weissig, H., Shindyalov, I.N., Bourne, P.E., 2000. The protein data bank. Nucleic Acids Res. 28 (1), 235–242.

Bhosale, U.A., Yegnanarayan, R., Pophale, P., Somani, R., 2012. Effect of aqueous extracts of Achyranthes aspera Linn. on experimental animal model for inflammation. Ancient Sci. Life 31, 202–206. https://doi.org/10.4103/0257-7941.107362.

Bostancikliogl u, S.M., Temiz, E., 2020. Severe acute respiratory syndrome coronavirus 2 is penetrating to dementia research. Curr. Neurovascular Res. 1–5.

Brockmeier, S.L., Lager, K.M., 2002. Experimental airborne transmission of porcine reproductive and respiratory syndrome virus and Bordetella bronchiseptica. Vet. Microbiol. 89 (4), 267–275.

Chen, Z.L., Zhang, W.J., Lu, Y., Guo, C., Guo, Z.M., Liao, C.H., Zhang, X., Zhang, Y., Han, X.H., Li, Q.L., Lu, J.H., 2020. From SARS-CoV to 2019-nCoV outbreak: similarities in the early epidemics and prediction of future trends. Chinese Med J 133 (9), 1112–1114.

Cousins, R.K., 2005. ChemDraw ultra 9.0. CambridgeSoft, 100 CambridgePark drive. J. Am. Chem. Soc. 127 (11), 4115–4116. https://doi.org/10.1021/ja0410237. Cambridge, MA 02140. www.cambridgesoft.com.

Cowley, J.A., Dimmock, C.M., Spann, K.M., Walker, P.J., 2000. Gill-associated virus of Penaeus monodon prawns: an invertebrate virus with ORF1a and ORF1b genes related to arteri-and coronaviruses. J. Gen. Virol. 81 (6), 1473–1484.

He, L., Hou, J., Gan, M., et al., 2008. Cadinane sesquiterpenes from the leaves of Eupatorium adenophorum. J. Nat. Prod. 71 (8), 1485–1488. https://doi.org/10.1021/np800242w.

Jin, Y., Hou, L., Zhang, M., Tian, Z., Cao, A., Xie, X., 2014. Antiviral activity of *Eupatorium adenophorum* leaf extract against tobacco mosaic virus. Crop Protect. 60, 28–33.

Kirchdoerfer, R.N., Ward, A.B., 2019. Structure of the SARS-CoV nsp12 polymerase bound to nsp7 and nsp8 co-factors. Nat. Commun. 10 (1), 1–9.

Kjær, J., Belsham, G.J., 2018. Modifications to the foot-and-mouth disease virus 2A peptide: influence on polyprotein processing and virus replication. J. Virol. 92 (8).

Lu, C.C., Chen, M.Y., Lee, W.S., Chang, Y.L., 2020. Potential therapeutic agents against COVID-19: what we know so far. J. Chin. Med. Assoc. 1–3 https://doi.org/10.1097/JCMA.0000000000000318.

Ma, Q.P., Cheng, C.R., Li, X.F., Liang, X.Y., Ding, J., 2015. Chemistry, pharmacological activities and analysis of Ageratina adenophora. Asian J. Chem. 27, 4311–4316.

Magrone, T., Magrone, M., Jirillo, E., 2020. Focus on receptors for coronaviruses with special reference to angiotensin-converting enzyme 2 as a potential drug target-a perspective. Endocrine, Metabolic & Immune Disorders-Drug Targets (Formerly Current Drug Targets-Immune. Endocrine & Metabolic Disorders) 20 (6), 807–811.

Malik, Y.A., 2020. Properties of coronavirus and SARS-CoV-2. Malays. J. Pathol. 42 (1), 3–11.

NCT04382391, 2020. Study assessing vagus nerve stimulation in covid-19 respiratory symptoms. https://clinicaltrials.gov/show/NCT04382391.
Neupane, N.P., Das, A.K., Singh, A.K., Verma, A., 2020. Off label medication to combat COVID-19: review Results to Date. Bentham Sci Coronaviruses 1, 1–2.
O'Boyle, N.M., Banck, M., James, C.A., Morley, C., Vandermeersch, T., Hutchison, G.R., 2011. Open Babel: an open chemical toolbox. J. Cheminf. 3 (1), 33.
Pathak, P., Novak, J., Naumovich, V., Grishina, M., Balkrishna, A., Sharma, N., Sharma, V., Potemkin, V., Verma, A., 2020. Polyphenolic rich extract of Oroxylum indicum alleviate β-glucuronidase activity via down-regulate oxidative stress: experimental and computational studies. Biocatalysis and Agricultural Biotechnology 29, 101804.
Poudel, R., Neupane, N.P., Mukeri, I.H., Alok, S., Verma, A., 2020. An updated review on invasive nature, phytochemical evaluation, & pharmacological activity of Ageratina Adenophora, 11, pp. 2510–2520. https://doi.org/10.13040/IJPSR.0975-8232.11(6).2510-20, 6.
Robb, N.C., Smith, M., Vreede, F.T., Fodor, E., 2009. NS2/NEP protein regulates transcription and replication of the influenza virus RNA genome. J. Gen. Virol. 90 (6), 1398–1407.
Sahai, R., Dutta, S., Kumar, T., 2020. Anticoagulants in COVID-19 therapy: an evidence-based review. Int. J. Pharmaceut. Sci. Rev. Res. 63 (1), 191–195.
Tian, H., Liu, Y., Li, Y., Wu, C.H., Chen, B., Kraemer, M.U., Li, B., Cai, J., Xu, B., Yang, Q., Wang, B., 2020. An investigation of transmission control measures during the first 50 days of the COVID-19 epidemic in China. Science 368 (6491), 638–642.
Tskhay, A., Yezhova, A., Alibek, K., 2020. COVID-19 pandemic: is chronic inflammation a major cause of death? medRxiv 1–16. https://doi.org/10.1101/2020.05.12.20099572.
Wan, Y., Shang, J., Graham, R., Baric, R.S., Li, F., 2020. Receptor recognition by the novel coronavirus from wuhan: an analysis based on decade-long structural studies of SARS coronavirus. J. Virol. 94 (7), 1–9. https://doi.org/10.1128/jvi.00127-20.
Weiss Susan, R., 2005. Coronavirus pathogenesis and the emerging pathogen severe acute respiratory syndrome coronavirus/susan R. Weiss, sonia navas-martin. Microbiol. Mol. Biol. Rev. 69 (4), 635–664.
World Health Organization, 2020. Modes of Transmission of Virus Causing COVID-19: Implications for IPC Precaution Recommendations: Scientific Brief. World Health Organization, p. 27. March 2020 (No. WHO/2019-nCoV/Sci_Brief/Transmission_modes/2020.1.
Worldometers, 2020. Coronavirus cases. Retrieved November 27. https://www.worldometers.info/coronavirus/.
Wu, R., Wang, L., Kuo, H.C.D., Shannar, A., Peter, R., Chou, P.J., Li, S., Hudlikar, R., Liu, X., Liu, Z., Poiani, G.J., 2020. An update on current therapeutic drugs treating COVID-19. Current Pharmacology Reports 1.
Yang, H., Yang, M., Ding, Y., Liu, Y., Lou, Z., Zhou, Z., Sun, L., Mo, L., Ye, S., Pang, H., Gao, G.F., 2003. The crystal structures of severe acute respiratory syndrome virus main protease and its complex with an inhibitor. Proc. Natl. Acad. Sci. Unit. States Am. 100 (23), 13190–13195.
Zhu, L., Sun, O.J., Sang, W., Li, Z., Ma, K., 2007. Predicting the spatial distribution of an invasive plant species (Eupatorium adenophorum) in China. Landsc. Ecol. 22 (8), 1143–1154.
Zoete, V., Daina, A., Bovigny, C., Michielin, O., 2016. Swiss similarity: a web tool for low to ultra high throughput ligand-based virtual screening. J. Chem. Inf. Model. 56 (8), 1399–1404. https://doi.org/10.1021/acs.jcim.6b00174.